Hindawi Publishing Corporation
EURASIP Journal on Audio, Speech, and Music Processing
Volume 2010, Article ID 928439, 11 pages
doi:10.1155/2010/928439

Research Article

Optimizing the Directivity of Multiway Loudspeaker Systems

Hmaied Shaiek (EURASIP Member)[1] and Jean Marc Boucher[2]

[1] *École Nationale d'Ingénieurs de Brest, Université Européenne de Bretagne (UEB), Laboratoire Brestois de Mécanique et des Systèmes (LBMS), EA 4325, Technopôle Brest-Iroise, CS 73862, 29238 Brest Cedex 3, France*
[2] *TELECOM Bretagne, Institut TELECOM, Université Européenne de Bretagne (UEB), CNRS UMR 3192 Lab-STICC, CS 83818, 29238 Brest Cedex 3, France*

Correspondence should be addressed to Hmaied Shaiek, shaiek_hmaied@yahoo.fr

Received 26 March 2010; Revised 8 July 2010; Accepted 19 August 2010

Academic Editor: Woon Seng Gan

In multiway loudspeaker systems, digital signal processing techniques have been used to correct the frequency response, the propagation time, and the lobbing errors. These solutions are mainly based on correcting the delays between the signals coming from loudspeaker system transducers, and they still show limited performances over the overlap frequency bands. In this paper, we propose an enhanced optimization of relevant directivity characteristics of a multiway loudspeaker system such as the frequency response, the radiation pattern, and the directivity index over an extended transducers' frequency overlap bands. The optimization process is based on applying complex weights to the crossover filter transfer functions by using an iterative approach.

1. Introduction

As full-range transducer designed to have the widest frequency band with a good overall performance is hard to achieve, most high-quality loudspeaker systems are of the multiway type. Therefore, two or more drive units must be used, each one of them being designed for a limited frequency range. In such acoustic source, we must avoid band aliasing and prevent each transducer from being fed with signals outside its frequency band. Thus, a suitable filter bank must be employed to split the input signal into different bands. This network is known as loudspeaker crossover [1–3].

When transducers have a separate geometrical distribution, the crossover design is generally done for a particular on-axis listening point, by including extra delays to correct the differences between the propagation time of the sound waves coming from all the transducers [1, 4]. Alternatively, the D'Appolito geometrical distribution [5] or the psychoacoustic error cancelation [6] could be used to reach this target over a wider listening area. With such solution, some amplitude, phase and directivity deviations still remain around the crossover frequencies when the listener moves away from the central listening point. In [7], it was shown that the best solution to control the directivite behavior of a multiway loudspeaker system is to mount its transducers around the same axis and use a coaxial configuration.

For a high-end loudspeaker system, the fluctuation of the directivity characteristics are sometimes unacceptable [8, 9]. These parameters are function of the crossover filter transfer functions especially over the transducers' overlap bands. In this paper, we will introduce a dedicated signal processing technique based on a complex weighting of the crossover filter responses in order to optimize relevant directivity parameters.

This paper is organized in two main sections. The first one introduces the technique that we propose to enhance the control of relevant directivity parameters for a multiway loudspeaker system. This control is achieved through a complex weighting of the crossover filter frequency responses over the transducers' overlap bands. In the second section of this paper, we will discuss the results of an application example, based on measurements done with a Cabasse (http://www.cabasse.com/) two-way coaxial loudspeaker system.

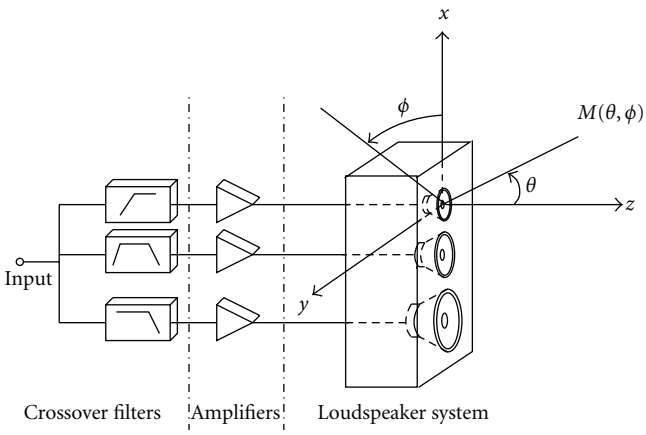

Figure 1: Multiway active loudspeaker system.

2. Proposed Algorithm

2.1. Notations. For a multiway loudspeaker system, such as that one shown in Figure 1, we introduce the following notations:

(i) $h_k(\theta, \phi, f)$: transfer function of the kth transducer measured at a listening point $M(\theta, \phi)$, one meter away from the top transducer (generally reproducing the high frequencies: tweeter);

(ii) $b_k(f)$: transfer function of the crossover filter applied to the kth transducer.

Let $A(\theta, \phi, f)$ and $W(f)$ be the $K \times 1$ vectors given by

$$A(\theta, \phi, f) = [h_1(\theta, \phi, f) b_1(f), \ldots, h_K(\theta, \phi, f) b_K(f)]^T,$$
$$W(f) = [w_1(f), \ldots, w_K(f)]^T, \tag{1}$$

where $A(\theta, \phi, f)$ is the vector containing the filtered transducers' transfer functions. For $(\theta, \phi) = (0, 0)$, the vector A contains the axially filtered transducer responses and will be noted $A_{\text{axis}}(f)$. $W(f)$ is the vector containing the complex frequency weights to be applied to transducer $1, \ldots, K$. In (1), $(\cdot)^T$ denotes the transpose operator.

The aim of our method is to find the optimal weights $w_k(f)$, $k = 1, \ldots, K$ that optimize suited directivity characteristics of a given multiway loudspeaker system.

2.2. Loudspeaker Directivity Characteristics. Assuming a spherical wave radiation, the directional factor of the multiway loudspeaker system is given by

$$\text{DF}(\theta, \phi, f) = \left| \frac{A^H(\theta, \phi, f) W(f)}{A^H_{\text{axis}}(f) W(f)} \right|, \tag{2}$$

where $|\cdot|$ is the modulus operator and $(\cdot)^H$ denotes the complex conjugate transpose operator.

The directivity of the loudspeaker system can then be approached by [10]

$$D(f) = \frac{W^H(f) E(f) W(f)}{W^H(f) L(f) W(f)}, \tag{3}$$

where $E(f)$ and $L(f)$ are $K \times K$ matrices given by

$$E(f) = A_{\text{axis}}(f) A^H_{\text{axis}}(f),$$
$$L(f) = \frac{1}{4\pi} \int_{\theta=0}^{\pi} \int_{\phi=0}^{2\pi} A(\theta, \phi, f) A^H(\theta, \phi, f) \sin(\theta) d\theta \, d\phi. \tag{4}$$

The directivity index of the filtered loudspeaker system is then given by

$$\text{DI}(f) = 10 \log_{10}(D(f)), \tag{5}$$

where $\log_{10}(\cdot)$ is the decimal logarithm function.

2.3. Cost Function. The proposed algorithm for optimizing the crossover filter bank of a multiway loudspeaker system is based on antenna array filtering techniques [11]. For this system, the synthesis of the radiation pattern is generally based on finding the weights that produce a predefined polar response. The principle of this synthesis is equivalent to minimizing a Hermitian criterion on the differences between the radiation pattern of the weighted system and a given target.

For our context, we seek to control the radiation of a multiway loudspeaker system over the transducers' overlap frequency bands. Our goal is to ensure a progressive directivity, in the vertical plane ($\phi = 0$) orthogonal to transducers' membranes, by forcing N directions $(\theta_n, \phi = 0)$, $n = 1, \ldots, N$ of the radiation pattern (2) to positive gains $g_n(f)$. This criterion can be achieved by minimizing the following cost function:

$$J(W) = \sum_{n=1}^{N} \left(\left| A^H(\theta_n, 0, f) W(f) \right| - g_n(f) \left| A^H_{\text{axis}}(f) W(f) \right| \right)^2. \tag{6}$$

The control of the radiation pattern in various directions requires the choice of fixed gains $g_n(f)$ for the corresponding angles. This gain can be the same for all the frequencies of the overlap band. Otherwise it can be a decreasing function with frequency according to loudspeaker system directivity.

In the case of a multiway loudspeaker system the control of the radiation pattern is done for few directions. As a first constraint, the cost function must take into account the fluctuations of the radiated acoustic power over overlap frequency bands. This can be reached by minimizing the fluctuations of the directivity index of the multiway loudspeaker system around an average target response $\text{DI}_{\text{av}}(f)$. As a second constraint the optimization process should not induce important amplitude fluctuations over the axial response of the multiway loudspeaker system. Taking into

account these constraints, the cost function to be minimized can be rewritten as follows:

$$J(W,\alpha,\beta) = \sum_{n=1}^{N}\left(\left|A^H(\theta_n,0,f)W(f)\right| - g_n(f)\left|A^H_{\text{axis}}(f)W(f)\right|\right)^2 + \alpha\left(\left|A^H_{\text{axis}}(f)W(f)\right| - 1\right)^2 + \beta\left|W^H(f)P(f)W(f)\right|^2, \quad (7)$$

where $P(f) = E(f) - \sigma(f)L(f)$, $\sigma(f) = e^{0.23\text{DI}_{\text{av}}(f)}$ and $e(\cdot)$ is the exponential function. In (7) α and β are two Lagrange multipliers.

The cost function to be minimized is thus a weighted sum of the following components:

(1) $\sum_{n=1}^{N}(|A^H(\theta_n,0,f)W(f)| - g_n(f)|A^H_{\text{axis}}(f)W(f)|)^2$: to *control the radiation pattern* of the loudspeaker system in N directions,

(2) $(|A^H_{\text{axis}}W(f)| - 1)^2$: to *control the axial response* of the loudspeaker system and avoid excessive amplitude weights,

(3) $|W^H(f)P(f)W(f)|^2$: to *control the directivity index* of the loudspeaker system in order to avoid unacceptable fluctuations of the radiated acoustic power over transducers overlap bands.

2.4. Determination of the Optimal Weights. The cost of (7) is more complicated than a cost on the complex terms: $\sum_n (A^H(\theta_n,0,f)W(f) - g_n(f))^2$ where the optimal solutions on $|A^H(\theta_n,0,f)W(f)| = g_n(f)$ (2^N for $n = 1,\ldots,N$) are symmetrical compared to the the origin. However, $J(W,\alpha,\beta)$ is differentiable according to $w_1(f),\ldots,w_K(f)$: components of the vector $W(f)$. We can so calculate the gradient and use an iterative optimization method which gives approximated numerical solutions of the optimal weights to be applied to the crossover filter transfer functions.

Let $R(f)$ and $Q(f)$ be the $N \times 1$ vectors given by

$$R(f) = \left[\left|A^H(\theta_1,0,f)W(f)\right| \cdots \left|A^H(\theta_N,0,f)W(f)\right|\right]^T,$$
$$Q(f) = \left[g_1(f)\left|A^H_{\text{axis}}(f)W(f)\right| \cdots g_N(f)\left|A^H_{\text{axis}}(f)W(f)\right|\right]^T. \quad (8)$$

By using the previous notations we can rewrite (7) as follows:

$$\begin{aligned} J(W,\alpha,\beta) &= (R(f) - Q(f))^2 + \alpha\left(\left|A^H_{\text{axis}}(f)W(f)\right| - 1\right)^2 + \beta\left|W^H(f)P(f)W(f)\right|^2 \\ &= |R(f)|^2 + |Q(f)|^2 - 2Q(f)^T R(f) + \alpha\left(\left|A^H_{\text{axis}}(f)W(f)\right| - 1\right)^2 + \beta\left|W^H(f)P(f)W(f)\right|^2. \end{aligned} \quad (9)$$

The gradient $\vec{\nabla}_W J(W,\alpha,\beta)$ of the cost function $J(W,\alpha,\beta)$ (developed in the appendix) is given by

$$\begin{aligned} \vec{\nabla}_W J(W,\alpha,\beta) &= \frac{\partial J(W,\alpha,\beta)}{\partial W^*} = \left(Y(f)Y^H(f) + X(f)X^H(f)\right)W(f) \\ &\quad - Y(f)\left[U(f)\odot Y^H(f)\right]W(f) \\ &\quad - X(f)\left[V(f)\odot X^H(f)\right]W(f) \\ &\quad + \alpha\left(1 - \frac{1}{\left|A^H_{\text{axis}}(f)W(f)\right|}\right)A_{\text{axis}}(f)A^H_{\text{axis}}(f)W(f) \\ &\quad + 2\beta W^H(f)P(f)W(f)P(f)W(f), \end{aligned} \quad (10)$$

where $\partial J(W,\alpha,\beta)/\partial W^*$ denotes the vector of the partial derivative of $J(W,\alpha,\beta)$ with respect to the components of the vector W^*, $(\cdot)^*$ denotes the complex conjugate operator and $\odot$ denotes the term-by-term Hadamard product. Matrices $X(f)$ and $Y(f)$ are of dimension $K \times N$ and they are given by

$$\begin{aligned} X(f) &= [A(\theta_1,0,f),\ldots,A(\theta_N,0,f)], \\ Y(f) &= [g_1(f)A_{\text{axis}}(f),\ldots,g_N(f)A_{\text{axis}}(f)]. \end{aligned} \quad (11)$$

In (10), $U(f)$ and $V(f)$ are the $N \times K$ matrices given by

$$\begin{aligned} U(f) &= [Q(f)./R(f),\ldots,Q(f)./R(f)], \\ V(f) &= [R(f)./Q(f),\ldots,R(f)./Q(f)], \end{aligned} \quad (12)$$

where ./ denotes the term by term division.

For a given value of $W(f)$, the gradient $\vec{\nabla}_W J(W,\alpha,\beta)$ have a component which is opposite to the direction of the minimum. The algorithm of gradient descent [12] advances $W(f)$ in the opposite direction of the gradient and narrows it to the minimum. This algorithm is given by the following formula:

$$W^{m+1}(\alpha,\beta,f) = W^m(\alpha,\beta,f) - \mu\vec{\nabla}_W J(W^m(\alpha,\beta,f)), \quad (13)$$

where m is the number of iteration and μ is a step-size parameter introduced to control how far we can move along the error function surface at each iteration. If μ is large we can quickly reach the minimum but with bad precision. Conversely, if μ is small, the minimum is reached with better precision, but more slowly. Since no real-time constraint is imposed to the optimization process, we can use a small value for the step-size parameter μ and allow a large number of iteration to the gradient algorithm. This guarantees a better precision for the optimal weighting vector $W_{\text{opt}}(f)$. The complexity of this algorithm after M iteration amounts to $M(14K^2 + 11K + 8KN + N + 6)$ single instruction.

3. Application Example

3.1. Loudspeaker Systems with Separately Distributed Transducers. From (3), it can be seen that the determination of the directivity index for a multiway loudspeaker exhibits the knowledge of the system responses in all directions (θ, ϕ) over the 4π steradian. However, this becomes more complicated when using traditional loudspeakers with separately distributed transducers. Meyer [13] and Kenneth and Birkle [14] proposed the use of some interpolation techniques for the estimation of loudspeaker system response at any given direction. However these methods still show limited performances, for real applications because they are based on using simplified model radiators such as monopole or flat piston mounted in an infinite baffle.

3.2. Loudspeakers with Coaxially Mounted Transducers. In the case of coaxial loudspeaker systems [7] and based on axial symmetries (around the $[Oz)$ axis for the system of Figure 1), the expression of the matrix $L(f)$ in (3) used to characterize the directivity index of the system can be simplified to the following formula:

$$L(f) = \frac{1}{2}\int_{\theta=0}^{\pi} A(\theta, f)A^H(\theta, f)\sin(\theta)d\theta. \qquad (14)$$

Thus, for calculating the directivity index of a coaxial loudspeaker system we just need few measurements over 2π steradian.

3.3. Experimental Results. The algorithm described in the previous section will then be applied to enhance the control of the directivity characteristics of a Cabasse, two-way coaxial loudspeaker system shown in Figure 2.

This loudspeaker system consists of two transducers coaxially mounted in a closed box enclosure. The central dome with a convex shape is the tweeter of diameter 0.028 m surrounded by the medium concentric radiating ring with an outside diameter of 0.106 m and inside diameter of 0.043 m. The tweeter dome is loaded by a small waveguide which helps in assuring the continuity of shape with the medium drive unit and optimizes the polar pattern of the tweeter on its low-frequency range, especially on the overlap region with the medium [7]. This transducer has a conical shape on its center. As far as the periphery part is concerned, it turns to a convex shape in order to prevent diffraction effects.

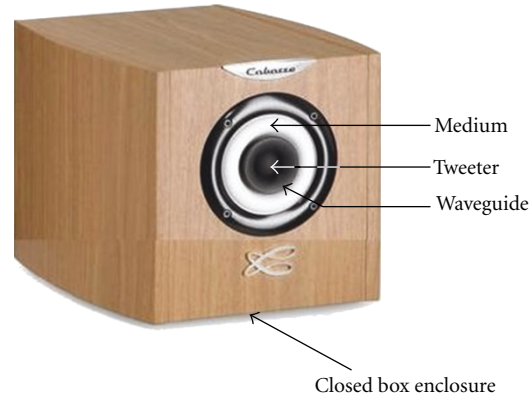

Figure 2: The Cabasse two-way coaxial loudspeaker system.

The measurements of the frequency responses necessary for determining the directivity characteristics of the loudspeaker system were made in an anechoic room of size $6 \times 7 \times 8\,\text{m}^3$. The block diagram of the measuring chain is given by Figure 3. In this diagram, a personal computer allows the generation and acquisition of the input and output signals needed to characterize the acoustic drivers. The determination of transducers' impulse responses is based on the Maximum Length Sequences (MLS) technique [15]. Another function of the personal computer is the control of the turntable on which lies the loudspeaker system. These functions are managed by the CLIOwin (http://www.audiomatica.com/home.htm) software. The input channel of a dedicated sound card is connected to a calibrated microphone (CLIO MIC-03, condenser electret, microphone) positioned at 1 m in front of the tweeter dome. The amplified signal of the sound card output channel is connected to the loudspeaker system input. Once a measurement is done, the turntable is shifted with 5°. Considering the loudspeaker system symmetry, only measurements between 0° and 180° are needed (14). All the measurement data are then exported in a usable format by the MATLAB (http://www.mathworks.com/) software. The experimental protocol described previously is applied separately to each transducer of the loudspeaker system.

The on-axis amplitude responses of the medium ($|h_1(0, 0, f)|$) and the tweeter ($|h_2(0, 0, f)|$) are depicted in Figure 4. We can identify the band-pass behavior of these transducers with a frequency band of [500 Hz, 4000 Hz] for the first drive unit and [4000 Hz, 20000 Hz] for the second one. The fluctuations in these amplitude responses are mainly due to diffraction effects and can be corrected by an adapted equalizer.

In practice, the width of the frequency overlap band do not exceed 2 octaves. This width takes into account the nonlinear behavior of the transducers. From the axial amplitude responses of the two transducers given in Figure 4, we can see an extended overlap frequency band ranging from 2000 Hz to 6000 Hz.

In this section we will also compare the performances of our method to a conventional one, such as, that one proposed by Vanderkooy and Lipshitz [4]. In this paper,

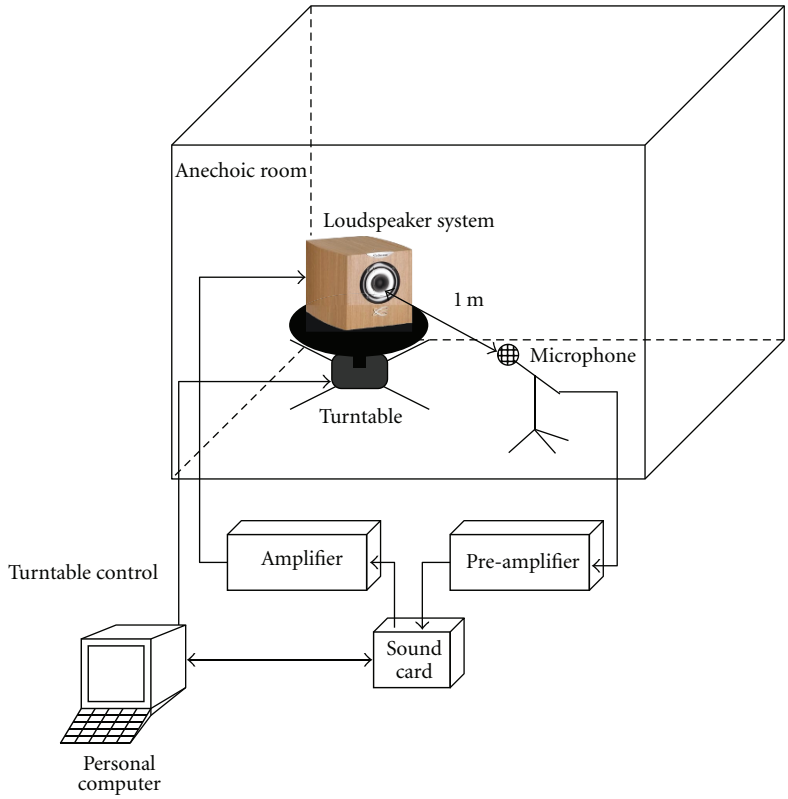

Figure 3: Experimental measurement protocol.

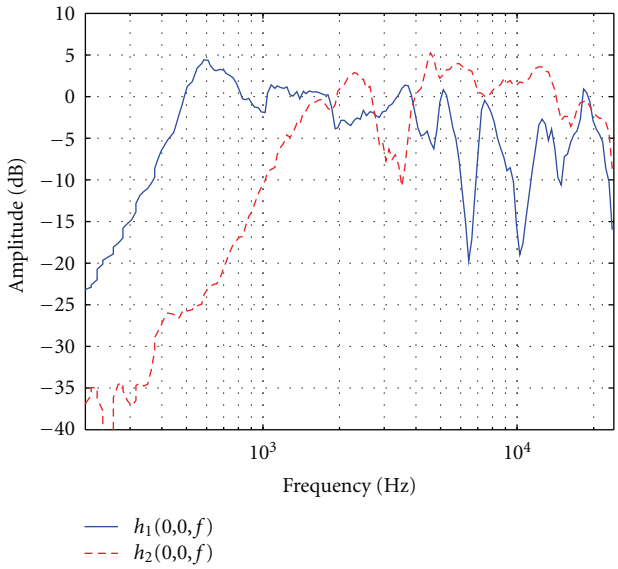

Figure 4: On-axis amplitude responses of the transducers.

the authors proposed the use of a pair of an in-phase squared Butterworth crossover filters. The amplitude and phase responses of these filters are shown in Figure 5.

The Butterworth filters have been designed to have a cutoff of 4000 Hz and moderate slopes of 24 dB/octave. With this crossover and since we are using a coaxial configuration for the multiway loudspeaker system, no extra processing is needed to correct the delays between the signals coming from the several transducers.

The crossover that we propose for the optimization process is a pair of low-pass (of order 14)/high-pass (of order 26), linear phase, finite impulse response filters. The amplitude and phase responses of these filters are shown in Figure 6. This filter bank have been designed to have the same cutoff frequency and slopes as the squared Butterworth filters shown in Figure 5.

For the optimization, we targeted the control of the radiation pattern at four directions $(\theta_1 = 15°, \phi = 0)$, $(\theta_2 = 30°, \phi = 0)$, $(\theta_3 = 45°, \phi = 0)$ and $(\theta_4 = 60°, \phi = 0)$. For a given angle θ_i $(n = 1, \ldots, N = 4)$, the gain $g_n(f)$, in (7), decreases linearly with frequency in order to achieve a radiation pattern that narrows when the frequency increases. The algorithm is stopped after $M = 2000$ iteration which leads to 296000 instruction. In order to achieve a good precision for the optimal weighting vector $W_{\text{opt}}(f)$, the step size μ can be chosen in the interval $[0.008, 0.01]$.

We considered the case where we give much more importance to the control of the directivity index than that of the radiation pattern and the axial response of the loudspeaker system. This choice means a uniformly radiated sound power over a wider listening area. In this case, we adjust the Lagrange multipliers to $\alpha = 1$ and $\beta = 100$. In this paper we have not developed a study on an optimal choice

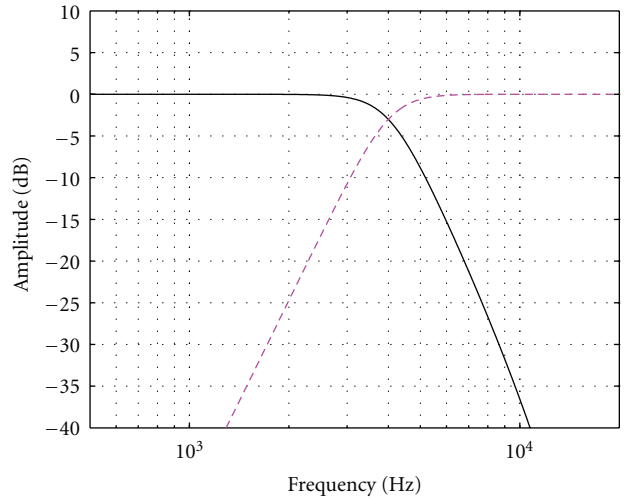

(a) *amplitude responses*

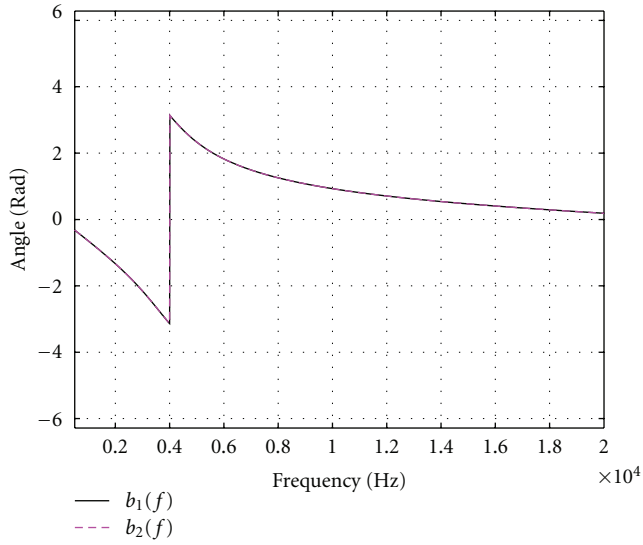

(b) *phase responses*

Figure 5: Frequency responses of the squared Butterworth crossover filters.

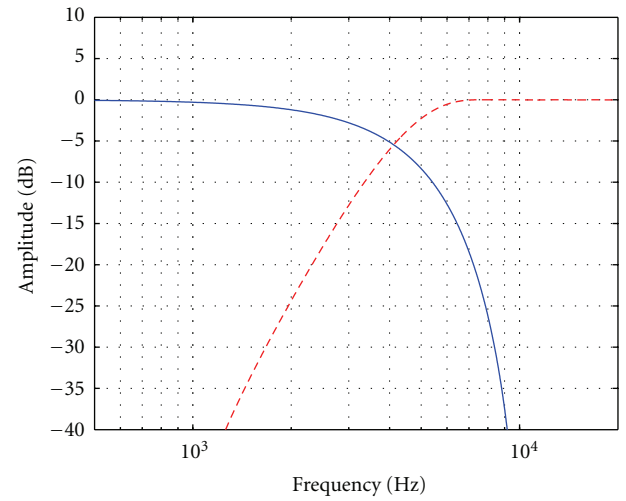

(a) *amplitude responses*

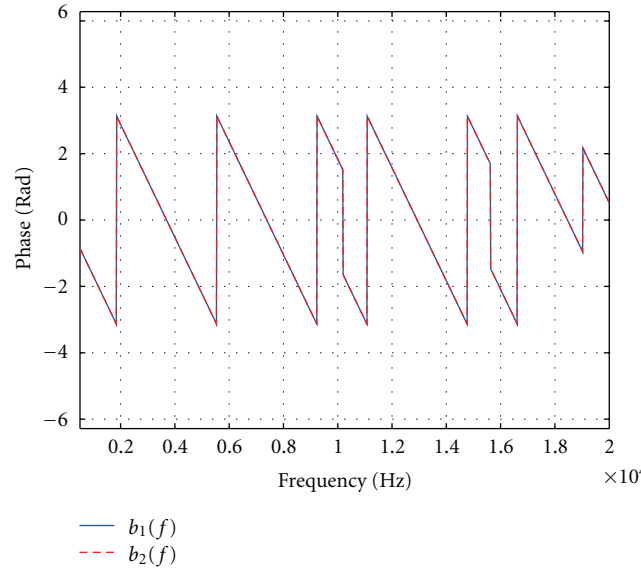

(b) *phase responses*

Figure 6: Frequency responses of the linear-phase crossover filters.

of parameters α and β. Indeed, the choice has been done systematically according to the importance we want to give to each directivity criterion.

The amplitude responses of the original and weighted linear-phase crossover filters are shown in Figure 7(a). The optimization process modifies the amplitude of the original filters over the frequency band of interest without adding high level gains. Figure 7(b), depicts the group delay $\tau_{g_1}(f)$ and $\tau_{g_2}(f)$ of the weighting filters $w_1(f)$ and $w_2(f)$. These delays are analytically given by

$$\tau_{g_k}(f) = -\frac{1}{2\pi}\frac{\partial \Phi_{w_k(f)}}{\partial f}, \tag{15}$$

where $\Phi_{w_k(f)}$ is the phase of the weighting filter $w_n(f)$ with $k = 1$ or $k = 2$.

As shown in Figure 7(b), the fluctuation of the group delay for the weighting filters, $w_1(f)$ and $w_2(f)$, do not exceed 1 ms which, according to Blauert and Laws [16], should not induce audible effects.

The directivity characteristics of the multiway loudspeaker system are given in Figures 8, 9, and 10. The radiation patterns of the loudspeaker system at 3 frequencies ($f = 3000$ Hz, $f = 4000$ Hz, and $f = 5500$ Hz) of the overlap region are given in Figure 8. As a first conclusion we remark a well controlled directivity compared to the case of the nonoptimized crossover filters or the case of using the conventional squared-Butterworth crossover filters. Indeed, with the optimization process, the main lobe of the multiway loudspeaker system narrows as the frequency increases. The second conclusion that we can notice is that the conventional method do not modify the radiation pattern of

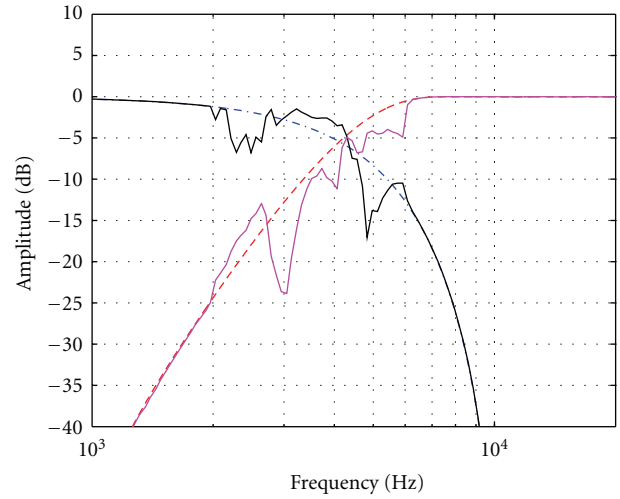

(a) *amplitude responses*

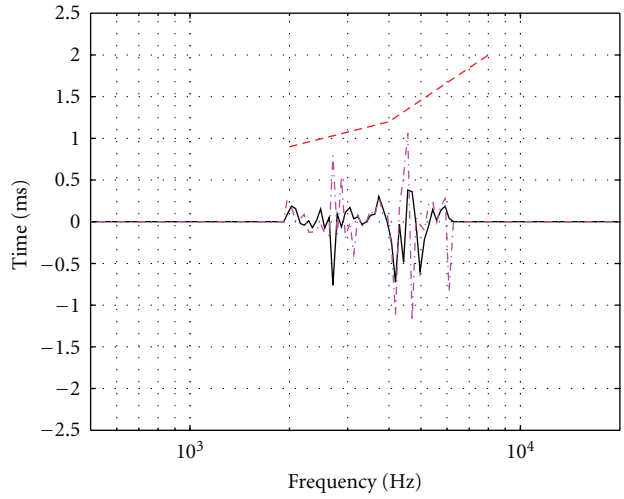

(b) *group delay*

FIGURE 7: Frequency responses of the optimized crossover filters.

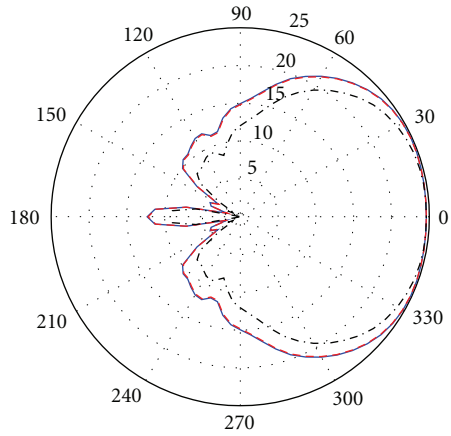

(a) $f = 3000$ Hz

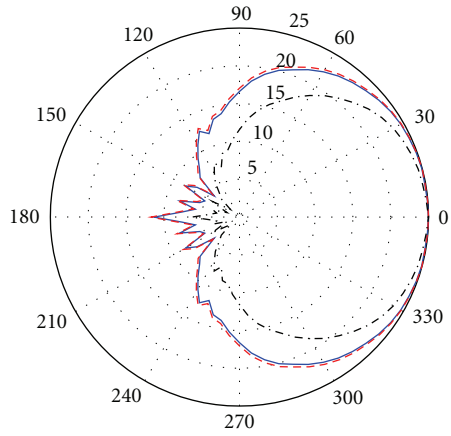

(b) $f = 4000$ Hz

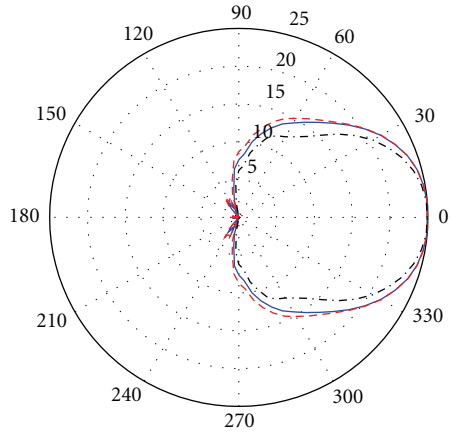

(c) $f = 5500$ Hz

FIGURE 8: Radiation pattern of the multiway loudspeaker system.

the loudspeaker system because, for each crossover network (the linear-phase, finite impulse response crossover and the squared Butterworth one), the filters used are in phase.

In Figure 9, we show the amplitude responses of the two-way coaxial loudspeaker system at 0°, 30°, and 60°. From Figures 9(a), 9(b), and 9(c), we observe that the optimization of crossover filters provides a steady decrease over the amplitude response of the loudspeaker system as we move away from its central axis. At this step, we can also underline the advantages of using a linear-phase, finite impulse responses filter bank over a squared Butterworth one. In fact, with a conventional filtering using a squared Butterworth crossover, an undesirable boost over the amplitude response of the

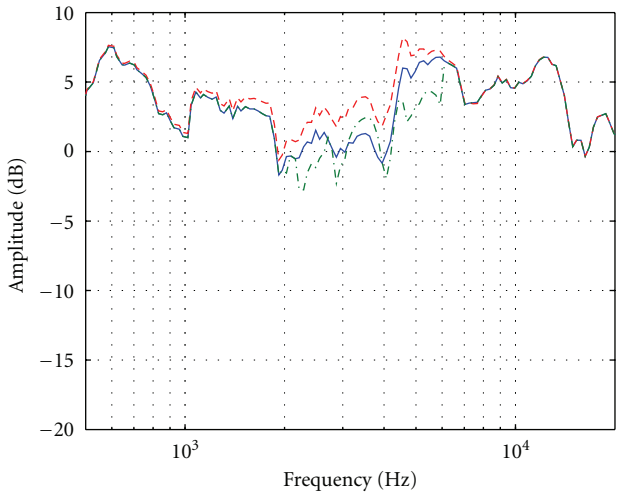

(a) 0°

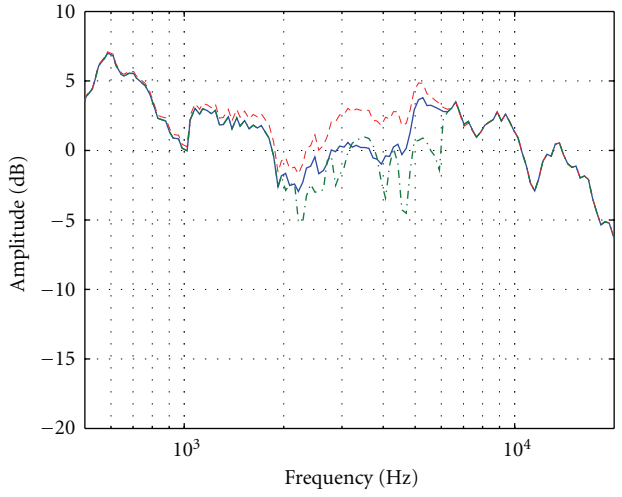

(b) 30°

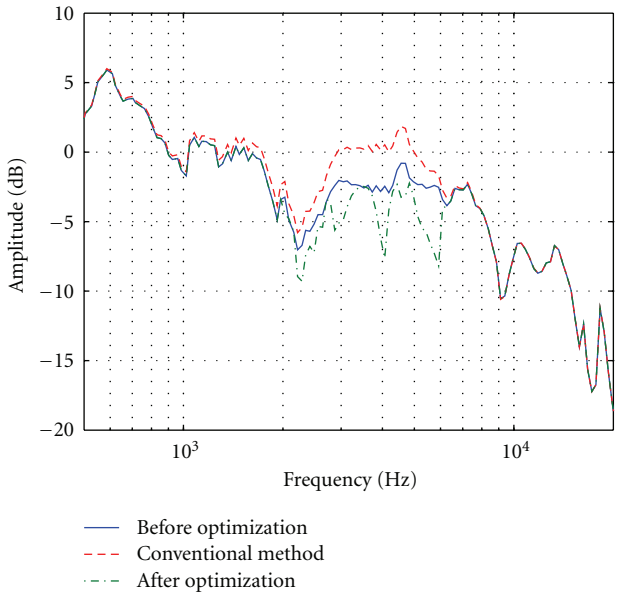

(c) 60°

Figure 9: Amplitude responses of the multiway loudspeaker system.

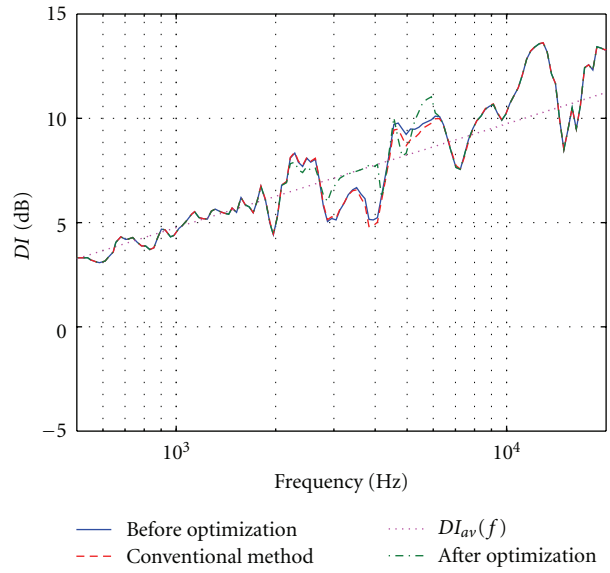

Figure 10: Directivity index of the multiway loudspeaker system.

loudspeaker system still remain over [3000 Hz, 5000 Hz] frequency band and even 60° away from the central axis of the loudspeaker system.

Regarding the directivity index, given in Figure 10, we see an improvement in the behavior of the radiated sound power after the weighting of the linear-phase, finite impulse response crossover filters. Indeed, with the optimization process, we have less fluctuations over the directivity index of the loudspeaker system as we move from the medium to the tweeter. We also remind that the in-phase behavior of the two filter banks used justifies the similarity between the directivity index of the loudspeaker system before the optimization of the linear-phase, finite impulse response crossover filters and when using a squared Butterworth crossover network.

4. Conclusion

In order to correct the frequency response or the lobbing errors of a multiway loudspeaker system, most solutions [1, 4] are based on delaying the signals sent to the loudspeaker system transducers. These solutions failed in achieving a uniformly radiated sound field especially when the transducers of the loudspeaker system are separately distributed.

In this paper, we have shown that, a dedicated complex weighting of the crossover filter responses, jointly optimizes the frequency response, the radiation pattern and the directivity index of the loudspeaker system over a wide frequency overlap band. Additionally, the performances obtained, are function of the degree of importance given to each radiation criterion through a judicious adjustment of Lagrange multipliers. The proposed method was then applied to enhance the control of the directivity behavior of a two-way coaxial loudspeaker system from the Cabasse company. In order to confirm its advantages, the performances of the proposed method were compared to a conventional crossover network

bank design [4] using a pair of in-phase squared Butterworth filters. Once the complex weights are obtained, the impulse responses of the optimized crossover filters can be obtained by using the generalized least squares method [17].

The method proposed in this paper can easily be applied to any frequency band. The interested reader can refer to [7] to get more information about the application of this technique to a three-way or a four-way loudspeaker system.

Appendix

Our aim is to calculate the gradient of the cost function $J(W,\alpha,\beta)$ given by(9)

$$\begin{aligned}\vec{\nabla}_W J(W,\alpha,\beta) &= \frac{\partial J(W,\alpha,\beta)}{\partial W^*} \\ &= \frac{\partial}{\partial W^*}\Big(|R(f)|^2 + |Q(f)|^2 - 2Q(f)^T R(f) \\ &\quad +\alpha\Big(\left|A_{\text{axis}}^H(f)W(f)\right| - 1\Big)^2 + \beta\left|W^H(f)P(f)W(f)\right|^2\Big).\end{aligned} \tag{A.1}$$

Let's calculate the gradient of each term in the previous equation:

(i) $\partial|R(f)|^2/\partial W^*(f) = ?$ and $\partial|Q(f)|^2/\partial W^*(f) = ?$

$$\begin{aligned}|R(f)|^2 &= \sum_{n=1}^{N}\left|A^H(\theta_n,0,f)W(f)\right|^2 \\ &= W^H(f)X(f)X^H(f)W(f),\end{aligned} \tag{A.2}$$

where $X(f)$ is the $K\times N$ matrix given by (11).

By the mean of complex matrices derivation formulas [11], we can write

$$\frac{\partial|R(f)|^2}{\partial W^*(f)} = X(f)X^H(f)W(f). \tag{A.3}$$

The same methodology applied to $|Q(f)|^2$ gives

$$\frac{\partial|Q(f)|^2}{\partial W^*(f)} = Y(f)Y^H(f)W(f), \tag{A.4}$$

where $Y(f)$ is the $K\times N$ matrix given by (11).

(ii) $\partial Q^T(f)R(f)/\partial W^*(f) = ?$

The scalar $Q^T(f)R(f)$ is the sum of N components.

$$\begin{aligned}Q^T(f)R(f) &= \sum_{n=1}^{N}\sqrt{g_n(f)\left|A_{\text{axis}}^H(f)W(f)\right|^2}\sqrt{|A^H(\theta_n,0,f)W(f)|^2} \\ &= \sum_{n=1}^{N} q_n r_n,\end{aligned} \tag{A.5}$$

where $q_n(f) = \sqrt{g_n(f)|A_{\text{axis}}^H(f)W(f)|^2}$ and $r_n(f) = \sqrt{|A^H(\theta_n,0,f)W(f)|^2}$.

For $n = 1,\ldots,N$:

$$\begin{aligned}&\frac{\partial q_n(f)r_n(f)}{\partial W^*(f)} \\ &= \frac{\partial\sqrt{g_n(f)\left|A_{\text{axis}}^H(f)W(f)\right|^2}\sqrt{|A^H(\theta_n,0,f)W(f)|^2}}{\partial W^*(f)} \\ &= \sqrt{g_n(f)\left|A_{\text{axis}}^H(f)W(f)\right|^2}\frac{\partial\sqrt{|A^H(\theta_n,0,f)W(f)|^2}}{\partial W^*(f)} \\ &\quad + \sqrt{|A^H(\theta_n,0,f)W(f)|^2}\frac{\partial\sqrt{g_n(f)\left|A_{\text{axis}}^H(f)W(f)\right|^2}}{\partial W^*(f)} \\ &= \frac{q_n(f)}{2r_n(f)}A(\theta_n,0,f)A^H(\theta_n,0,f)^H W(f) \\ &\quad + \frac{r_n(f)}{2q_n(f)}g_n(f)^2 A_{\text{axis}}(f)A_{\text{axis}}^H(f)W(f).\end{aligned} \tag{A.6}$$

The derivative of $Q^T(f)R(f)$ is then given by

$$\begin{aligned}&\frac{\partial Q^T(f)R(f)}{\partial W^*(f)} \\ &= \sum_{n=1}^{N}\frac{\partial q_n(f)r_n(f)}{\partial W^*(f)} \\ &= \left[\sum_{n=1}^{N}\frac{q_n(f)}{2r_n(f)}A(\theta_n,0,f)A^H(\theta_n,0,f)\right]W(f) \\ &\quad + \left[\sum_{n=1}^{N}\frac{r_n(f)}{2q_n(f)}g_n(f)^2 A_{\text{axis}}(f)A_{\text{axis}}^H(f)\right]W(f).\end{aligned} \tag{A.7}$$

Putting the last equation in a matrix form by using the notations of (10) leads to

$$\begin{aligned}\frac{\partial Q^T(f)R(f)}{\partial W^*(f)} &= \frac{1}{2}X(f)\left[V(f)\odot X^H(f)\right]W(f) \\ &\quad + \frac{1}{2}Y(f)\left[U(f)\odot Y(f)^H(f)\right]W(f),\end{aligned} \tag{A.8}$$

(iii) $\partial(|A_{\text{axis}}^H(f)W(f)| - 1)^2/\partial W^*(f) = ?$

By developing this term we obtain

$$\begin{aligned}\left(\left|A_{\text{axis}}^H(f)W(f)\right| - 1\right)^2 &= W(f)^H A_{\text{axis}}(f)A_{\text{axis}}^H(f)W(f) \\ &\quad - 2\left|A_{\text{axis}}^H(f)W(f)\right| + 1.\end{aligned} \tag{A.9}$$

For the first term of (A.9) we can write

$$\frac{\partial W^H(f)A_{\text{axis}}(f)A^H_{\text{axis}}(f)W(f)}{\partial W^*(f)} = A_{\text{axis}}(f)A^H_{\text{axis}}(f)W(f). \tag{A.10}$$

The derivative of $|A^H_{\text{axis}}(f)W(f)|$ with respect to the components of $W^*(f)$ is given by

$$\begin{aligned}\frac{\partial\left|A^H_{\text{axis}}(f)W(f)\right|}{\partial W^*(f)} &= \frac{\partial\sqrt{\left|A^H_{\text{axis}}(f)W(f)\right|^2}}{\partial W^*(f)}\\ &= \frac{\partial\sqrt{W^H(f)A_{\text{axis}}(f)A^H_{\text{axis}}(f)W(f)}}{\partial W^*(f)}\\ &= \frac{1}{2\sqrt{W^H(f)A_{\text{axis}}(f)A^H_{\text{axis}}(f)W(f)}}\\ &\quad\times\frac{\partial W^H(f)A_{\text{axis}}(f)A^H_{\text{axis}}(f)W(f)}{\partial W^*(f)}\\ &= \frac{1}{2\left|A^H_{\text{axis}}(f)W\right|}A_{\text{axis}}(f)A^H_{\text{axis}}(f)W(f).\end{aligned} \tag{A.11}$$

We obtain finally

$$\begin{aligned}&\frac{\partial\left(\left|A^H_{\text{axis}}(f)W(f)\right|-1\right)^2}{\partial W^*(f)}\\ &\quad=\left(1-\frac{1}{\left|A^H_{\text{axis}}(f)W(f)\right|}\right)A_{\text{axis}}(f)A^H_{\text{axis}}(f)W(f).\end{aligned} \tag{A.12}$$

(iv) $\partial(W^H(f)P(f)W(f))^2/\partial W^*(f) = ?$

The derivative of this composite function is relatively easy and is equal to

$$\frac{\partial(W^H(f)P(f)W(f))^2}{\partial W^*(f)} = 2W^H(f)P(f)W(f)P(f)W(f). \tag{A.13}$$

Finally the gradient of the cost function $J(W,\alpha,\beta)$ is given by

$$\begin{aligned}&\vec{\nabla}_W J(W,\alpha,\beta)\\ &\quad=\left(Y(f)Y^H(f)+X(f)X^H(f)\right)W(f)\\ &\quad-Y(f)\left[U(f)\odot Y^H(f)\right]W(f)\\ &\quad-X(f)\left[V(f)\odot X^H(f)\right]W(f)\\ &\quad+\alpha\left(1-\frac{1}{\left|A^H_{\text{axis}}(f)W(f)\right|}\right)A_{\text{axis}}(f)A^H_{\text{axis}}(f)W(f)\\ &\quad+2\beta W^H(f)P(f)W(f)P(f)W(f).\end{aligned} \tag{A.14}$$

Acknowledgments

This work was supported by Cabasse Acoustic Center. The authors would like to express special gratitude to Yvon KERNEIS, expert consultant at Cabasse Acoustics Center, Bernard DEBAIL, R&D director and Pierre-Yves DIQUELOU, project manager in the supporting company. The authors also wish to thank Emmanuel DELALEAU, professor at the École Nationale d'iNgénieurs de Brest, for various comments and interactions.

References

[1] R. Bews, *Digital crossover networks for active loudspeaker systems*, Ph.D. dissertation, University of Essex, Colchester, UK, 1987.

[2] K. C. Haddad, H. Stark, and N. P. Galatsanos, "Design of digital linear-phase fir crossover systems for loudspeakers by the method of vector space projections," *IEEE Transactions on Signal Processing*, vol. 47, no. 11, pp. 3058–3066, 1999.

[3] J. Baird and D. McGrath, "Practical application of linear phase crossovers with transition bands approaching a brick wall response for optimal loudspeaker frequency, impulse and polar response," in *Proceedings of the 115th Convention of the Audio Engineering Society*, New York, NY, USA, October 2003.

[4] J. Vanderkooy and S. P. Lipshitz, "Power response of loudspeakers with non-coincident drivers-the influence of crossover design," *Journal of the Audio Engineering Society*, vol. 34, no. 4, pp. 236–244, 1986.

[5] J. A. d'Appolito, "A geometric approach to eliminating lobbing error in multiway loudspeakers," in *Proceedings of the 74th Convention of the Audio Engineering Society*, New York, NY, USA, October 1983.

[6] A. Rimell, *Reduction of loudspeaker polar response aberrations through the application of psychoacoustic error concealment*, Ph.D. dissertation, Universityof Essex, Colchester, UK, 1996.

[7] H. Shaiek, *Optimizing wide band coaxial loudspeaker systems using digitalsignal processing techniques*, Ph.D. dissertation, TELECOM, Bretagne, France, 2007.

[8] N. Zacharov, "Subjective appraisal of loudspeaker directivity for multichannel reproduction," *Journal of the Audio Engineering Society*, vol. 46, no. 4, pp. 288–303, 1998.

[9] D. Queen, "The effect of loudspeaker radiation patterns on stereo imaging and clarity," *Journal of the Audio Engineering Society*, vol. 27, no. 5, pp. 358–379, 1979.

[10] L. E. Kinsler, A. R. Frey, A. B. Coppens, and J. V. Sanders, *Fundamentals of Acoustics*, John Wiley & Sons, New York, NY, USA, 4th edition, 2000.

[11] R. Lamberti, *Antenna array synthesis and pattern constrained adaptive beamforming*, Ph.D. dissertation, University of Orsay, Orsay, France, 1993.

[12] J. A. Snyman, *Practical Mathematical Optimization: An Introductionto Basic Optimization Theory and Classical and New Gradient-Based Algorithms*, Springer, Berlin, Germany, 2005.

[13] D. G. Meyer, "Computer simulation of loudspeaker directivity," *Journal of the Audio Engineering Society*, vol. 32, no. 5, pp. 294–314, 1984.

[14] J. D. Kenneth and T. K. Birkle, "Prediction of the full-space directivity characteristics of loudspeaker arrays," *Journal of the Audio Engineering Society*, vol. 38, no. 4, pp. 250–259, 1990.

[15] D. D. Rife and J. Vanderkooy, "Transfer-function measurement with maximum-length sequences," *Journal of the Audio Engineering Society*, vol. 37, no. 6, pp. 419–444, 1989.

[16] J. Blauert and P. Laws, "Group delay distortions in electroacoustical systems," *Journal of the Acoustical Society of America*, vol. 63, no. 5, pp. 1478–1483, 1978.

[17] T. I. Laakso, V. Välimäki, M. Karjalainen, and U. K. Laine, "Splitting the unit: delay tools for fractional delay filter design," *IEEE Signal Processing Magazine*, vol. 13, no. 1, pp. 30–60, 1996.